



Research Paper

Effect of Multi-staging in Vacuum Membrane Distillation on Productivity and Temperature Polarization

Waqas Alam, Muhammad Asif*, Wajeeha Bibi, Jawad Rabbi

Faculty of Mechanical Engineering, GIK Institute of Engineering Sciences and Technology, Topi, 23460, Pakistan

Article info

Received 2021-07-23
 Revised 2021-09-20
 Accepted 2021-10-17
 Available online 2021-10-17

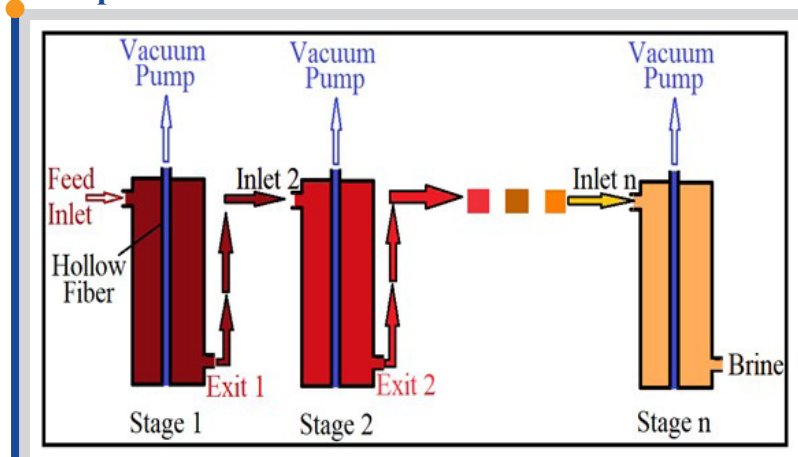
Keywords

Membrane distillation (MD)
 Vacuum MD (VMD)
 MSVMD
 Temperature polarization
 Multi-staging

Highlights

- Impact of multi-staging in VMD on productivity and temperature polarization
- Point of inversion in MSVMD is predicted
- Optimal number of stages in MSVMD
- Impact of process and membrane characteristics on TPC and productivity

Graphical abstract



Abstract

Multi-stage vacuum membrane distillation (MSVMD) has recently gained attention as means of enhancing the performance of single stage configuration. The present study is aimed to analyze the impact of multi-staging in VMD (vacuum membrane distillation) on productivity and the associated temperature polarization. Another goal is to determine the point of inversion, a point after which further multi-staging is no more beneficial both in terms of permeate productivity (flux) and associated temperature polarization. After validation with the experimental data, a parametric analysis of MSVMD performance is carried out numerically. Further, the permeate productivity and associated temperature polarization phenomenon were analyzed simultaneously under varying membrane specifications. The optimum number of stages, giving the maximum possible performance of MSVMD, is estimated for variation in most prominent process variables and membrane specifications. The point of inversion was found to be above 40 stages for varying process variables, however, it remained well below 20 stages for variation in some of the prominent membrane characteristics.

© 2022 FIMTEC & MPRL. All rights reserved.

1. Introduction

Water scarcity is one of the primary concerns that people throughout the world are dealing with, as it is a basic requirement of life on the planet [1]. Although, abundant resources of water on earth are available in the form of seawater, brackish water, lakes, glaciers, and underground water, however, only 0.75 percent of total water can be used directly for drinking purpose [2]. Recently, desalination has emerged as a best resource of finite freshwater, allowing it to be extracted from large quantities of saline water [3,4]. Desalination can be categorized on the basis of feed solution utilized (saltwater or brackish water), the type of separation process used (thermal or membrane), and the energy used to drive the desalination process.

Figure 1 presents the classification of desalination process on the basis of energy used to desalinate saline water. In thermal energy-based desalination,

membrane distillation (MD) is a cost-effective and innovative method of separating pure drinkable water from salty water [5]. MD processes are appealing because of their ability to be integrated with low-grade energy sources that require lower operating conditions, simple membrane construction, lower energy expenditure in the case of waste heat, nearly 100 percent salt rejection rate on paper, and their good capability to use low-grade energy sources [6,7]. Membrane distillation technology suffers from temperature polarization, concentration polarization, and heat loss from the permeable membrane itself, all of which negatively impact its performance. [8–10]. As shown in Figure 1, MD can be further classified into six different types. In DCMD, the heated feed solution and cold condensate are in direct contact with the permeable membrane on its opposite sides respectively. At

* Corresponding author: masif@giki.edu.pk (M. Asif)

the feed side, water molecules evaporate, flow across the permeable membrane, and condense at the other side. It has a high permeate flux but suffers from significant heat losses as a result of membrane conduction [11]. In AGMD, the porous membrane has a direct contact only on one side with the heated feed solution, however, on the other side the condensing surface and the membrane are separated by an air gap. The introduction of this air gap reduces the conduction heat losses in AGMD, however, this comes at the expense of reduced permeate flux [12]. In SGMD, an inert gas sweeps the vapor across the permeable membrane, where it condenses outside the membrane module. To effectively limit the heat loss and enhance mass transfer coefficient across the membrane, sweeping gas is kept mobile. The basic issue with SGMD is that a tiny proportion of permeate diffuses into a significant amount of sweep gas, costing a large condenser [13,14]. The process of VMD entails applying vacuum to the condensate side of the membrane, which must also be lower than the saturation pressure of the water solvent in the hot feed stream. Low pressure (vacuum) on the permeate side aids vapor flow through the membrane pores. For water recovery, external condenser is required in case of VMD [15]. TSGMD and LGMD are two hybrid MD configurations. TSGMD being a hybrid of AGMD and SGMD was developed to solve the problem of growing temperature along the membrane by placing a cold surface on the condensate side. Similarly, in order to solve the issue of high conduction heat loss, a hybrid of AGMD and DCMD was developed, known as LGMD. VMD as compared to other conventional MD designs, has an advantage of a higher distillate production rate due to the existence of vacuum on the permeate side, resulting in a stronger driving force (pressure gradient across the membrane). Another advantage of VMD is lower conduction heat loss due to the presence of vacuum gap. The vacuum level, on the other hand, should be kept under check because the liquid entry pressure (LEP) can exceed, resulting in membrane wetness [14,16]. Despite its many advantages over other MD processes, VMD is facing several challenges such as high specific heat consumption (SHC) and temperature polarization (TP). MD's widespread commercialization has been impeded by these two major flaws [17,18]. TP has a direct impact on the mechanism's driving power, causing a decrease in permeate productivity that results in poor system performance. In TP the bulk feed temperature T_b is decreased to feed inlet temperature T_i at the feed side membrane interface, due to the release of latent heat when water vapors evaporate, and heat is transported across the membrane.

The sensible heat energy of the exit stream in VMD module or the latent heat of condensation in permeate can be utilized to minimize the high specific heat consumption (SHC). Likewise, TP effect can be reduced by increasing the feed flow rate [19]. Moreover, averting direct contact between hot feed solution and the permeable membrane surface is the most dependable technique to eliminate the temperature polarization (TP) effect. By adopting this technique, the individual effects of mass transfer coefficient (MTC) and TP on the water vapor flux can be calculated easily [20]. If the exit stream of first VMD module is fed into another membrane unit, it can provide additional permeate flux that is obviously lower than the previous stage. Multi-stage membrane distillation is a system that consists of numerous stages of membrane units. VMD and AGMD have been used to construct a variety of multistage technologies. Gilron et al. [21] established a multistage DCMD process, which was then enhanced by his team [22] to improve the performance. Lu et al. [23] investigated the economics of a multi-stage AGMD process. Shim et al. [24] developed an MSVMD process with a GOR less than 1. Summers [25] developed MS-VMD, which is similar to MSF and has a GOR of 4. When compared to their single stage VMD process, it has a much lower specific heat consumption (SHC) [26]. Memsys, a company founded in 2009, created a new MD mechanism known as vacuum multi-effect membrane distillation (V-MEMD). These systems are reported to have a GOR of around 4 [27]. When based on a flat sheet membrane arrangement, Memsys VMD technology was reported to have a roughly 80% lower specific heat consumption SHC as compared to its original system. Likewise, several other scholars reported a decrease in the SHC for memsys-based systems [19,28]. In another research, Omar et al. [29] investigated the energy requirements and leveled cost of water (LCOW) for four different Multistage VMD process configurations. The results showed that a configuration with brine recirculation had the lowest energy consumption. Moreover, in terms of permeate productivity, the module packing density is also important. Despite decrease in SHC, the lower module packing density linked with flat sheet membrane systems limits permeate flux [30]. Hollow fiber membrane systems, as opposed to flat sheet membrane systems, have a significantly higher module packing density, leading to increased permeate flux [31–34]. Similarly, Kim et al. [35] presented a technical and economic analysis of multi-stage VMD coupled with solar energy. They analyzed the MSVMD for 28-stages and predicted the GOR of 47 and a leveled cost of 0.97 \$/m³.

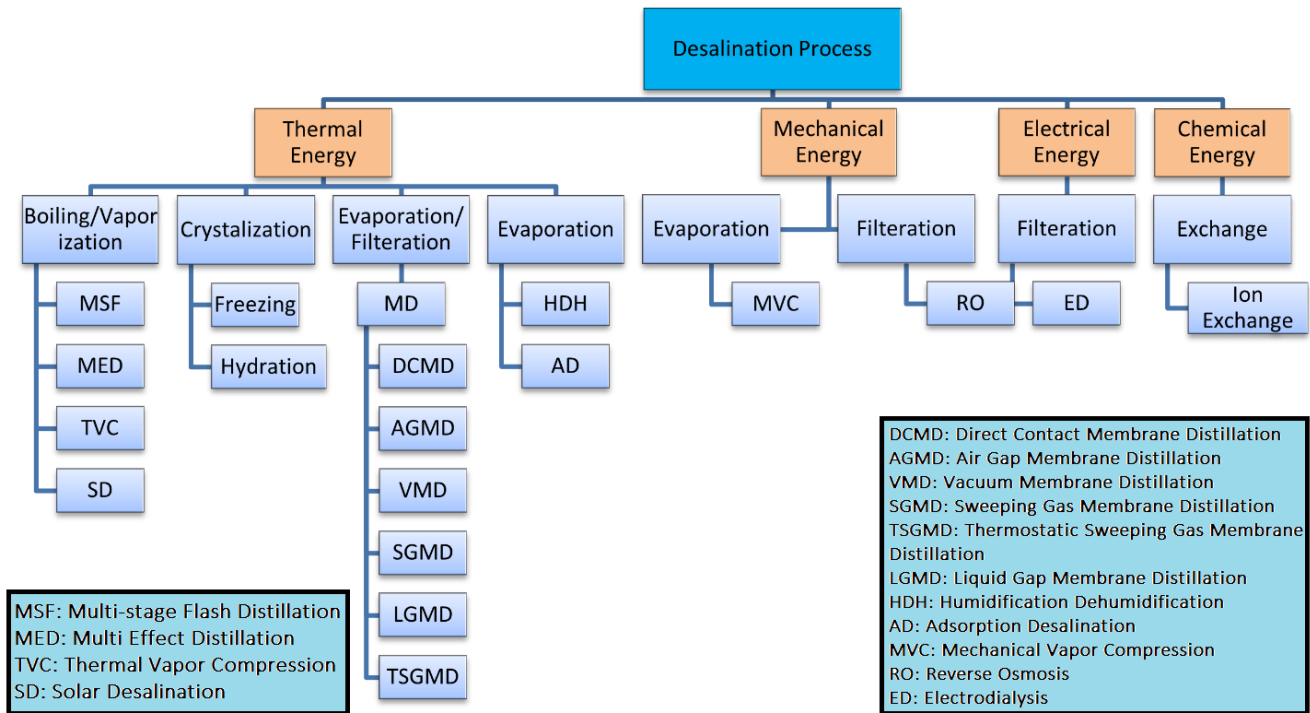


Fig. 1. Classification of desalination process based on type of energy input.

Because the MSVMD is a new concept, it has received relatively very little attention. Figure 2 depicts the number of research publications on single-stage VMD versus the number of articles published on MSVMD, on yearly basis between 2010 and 2020. It is evident that the first ever research article on MSVMD was reported in 2013, and there is currently very little literature on it. Following a thorough review of the previously published studies on MSVMD, it is discovered that only a few researchers have simultaneously investigated permeate productivity and associated temperature polarization as a function of various membrane characteristics. More importantly, no attempt has been made to determine the extent to which multi-staging is beneficial in terms of its overall performance. To the best of author's knowledge, MSVMD performance (permeate production) has never been critically analyzed as additional stages are added to the setup. Although the point of multi-staging is to operate at a lower driving force and draw out a higher permeate production (flux), however, every additional stage has some cost associated with it too. Therefore, the main intent of this study is to try and evaluate the point of inversion, a point after which further multi-staging is no more beneficial both in terms of permeate productivity and associated temperature polarization. Another objective is to analyze permeate productivity and associated temperature polarization phenomenon simultaneously, under varying membrane specifications. The optimum number of stages is estimated for the maximum possible performance of MSVMD under varying process variables and membrane specifications.

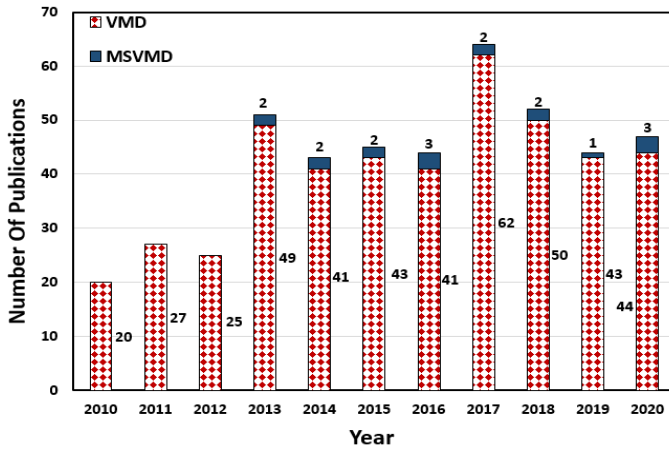


Fig. 2. Research activity on VMD and MSVMD 2010–20, (Source: Google Scholar).

1.1. Model for heat transfer

During the VMD process, heat transfer also takes place within the feed stream (from bulk to the membrane interface). This heat loss (via convection) can be evaluated as:

$$Q_f = h_f(\pi d_o N_f)(T_b - T_i) \quad (1)$$

where T_b is the temperature on bulk feed side, T_i denotes the feed side membrane interface temperature, d_o denotes the outer fibre diameter, N_f denotes the number of fibres in the shell, and h_f denotes the saline feed convective heat transfer coefficient. The term h_f can be evaluated by Groehen's equation [36]:

$$Nu = \frac{h_f d_h}{k_f} = 0.206(Re \cos\theta)^{0.63} Pr^{0.36} \quad (2)$$

where Re and Pr denote the Reynolds number and Prandtl number, respectively, d_h represents the shell hydraulic diameter, and θ represents the yaw angle, whose value varies between 0° for cross flow of feed stream to 90° for parallel flow of hot feed. The thermal conductivity of the feed stream is denoted by k_f . The above relationship holds true for $Re > 10000$.

One other type of heat transfer related with the VMD process is latent heat, which is transferred via vapors of permeate through the membrane pores. It can be computed by following expression.

$$Q_m = J g_v \quad (3)$$

where, g_v and J denote the saturated water enthalpy and permeate flux respectively.

Conduction heat loss through the membrane is negligible for membranes with a high porosity. In this case, the heat loss from the bulk of the hot feed stream to the interface between the feed solution and the membrane must be equal to the latent heat transferred via permeate vapors as they flow through the membrane pores [37]:

$$Q_f = Q_m \quad (4)$$

1.2. Model for mass transfer

Depending on a dimensionless number called the Knudsen number, the mass transfer of vapors across membrane pores obeys either the Knudsen diffusion model or the Poiseuille flow model. The Knudsen number is given by following expression:

$$k_n = \frac{\lambda}{L} \quad (5)$$

where,

λ = Mean free molecular path

L = characteristic length (mean pore size/diameter in flow through membrane pores)

A Knudsen number less than one indicates Poiseuille flow for a non-continuum model, whereas a Knudsen number greater than one indicates that mass transfer via the Knudsen diffusion model is dominant [37]. Usually, the mean free molecular path in VMD is substantially larger than the membrane pore size. Hence, Knudsen diffusion is the primary controller of mass transport across the membrane. In the case of the Knudsen diffusion model, the permeate mass flux is calculated using the following relationship:

$$J_k = 1.064 \frac{r\varepsilon}{\tau\delta} \left(\frac{M}{RT_{avg}} \right)^{0.5} (P_i - P_v) \quad (6)$$

where, $(P_i - P_v)$ denotes the vapor pressure drop across the membrane and τ , δ , r and ε denote the membrane tortuosity, thickness, mean pore size, and membrane porosity, respectively. The molecular weight of water, universal gas constant, and absolute temperature in membrane pores are represented by M , R and T_{avg} , respectively. The vacuum side pressure P_v is measured using a pressure gauge, and the water pressure at the feed side membrane interface P_i is computed by following expression:

$$P_i = P_w \times (1 - X) \quad (7)$$

where, X denotes the mole fraction of salt in the saline feed solution and P_w is determined via Antoine equation as:

$$P_w = 10^{\left(\frac{8.07131 - \frac{1730.63}{233.426 + T_i}}{1} \right)} \times 133.3 \text{ Pa} \quad (8)$$

1.3. MSVMD numerical model

Heat transfer and mass transfer are interrelated in a VMD process. When the process is in a steady state, the total energy and mass balance can be computed by following expression:

$$Q = h_f(T_b - T_i) = J g_v = C_m = 1.064 \frac{r\varepsilon}{\tau\delta} \left(\frac{M}{RT_{avg}} \right)^{0.5} (P_i - P_v) g_v \quad (9)$$

g_v denoting the vaporization enthalpy of feed stream, can be computed by using the following expression [38]:

$$g_v = (2501.689845 + 1.806916015T_i + 5.087717) \times 10^{-4} T_i^2 - (1.1221) \times 10^{-5} T_i^3 \quad (10)$$

The schematic of MSVMD setup adopted in this study is shown in Figure 3. Once a single stage VMD is solved, the parameters that change for the next stage are shown in Table 1.

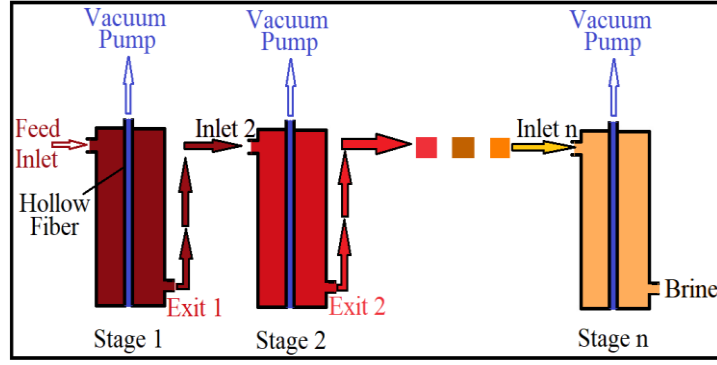


Fig. 3. Schematic of the MSVMD configuration utilized in current study.

Table 1

Variables that vary for successive stages.

Variables	Description
T_{fi}	Bulk Feed inlet temperature
Vol_{total}	Total volume of feed solution
Conc	Concentration of hot feed solution
X	Mole-fraction of salt in feed solution
M	Molecular weight of feed solution
P	Density of feed solution

All the other parameters remain constant for the successive stages. The above parameters are needed to be solved for each successive stage in order to solve the MSVMD mechanism numerically. The bulk feed inlet temperature for each stage in succession is found using energy balance for the predecessor stage. The total heat lost from the feed stream in a single stage can be expressed in the following form:

$$Q_{lost} = \dot{m}_f * c_p * (T_{fi} - T_{fe}) \quad (11)$$

where, \dot{m}_f is the mass flowrate of saline feed solution, C_p is the specific heat capacity of feed, and $(T_{fi}-T_{fe})$ represents the temperature drop in the bulk feed temperature as it passes through a single stage.

Since it is assumed that no heat is lost due to conduction through the membrane, it means that all this heat Q_{lost} is transferred via water permeate vapors onto the permeate side. Hence, at steady state condition, the heat lost from the bulk feed stream is equal to the heat transferred with the permeate flux. Therefore, it can be expressed as follow:

$$Q_{lost} = \dot{m}_f * c_p * (T_{fi} - T_{fe}) = J * g_v * A \quad (12)$$

The above relation can be used to solve for the bulk feed exiting temperature T_{fe} , which will be the bulk feed inlet temperature for the following stage.

The second model assumption which says that during the separation process no mass is produced or consumed is enough to find the remaining volume of feed solution after each stage of the process. It can be expressed as:

$$Vol_{total} = Vol_{initial} - Vol_{permeate} \quad (13)$$

where Vol_{total} represents the remaining volume after a stage, $Vol_{initial}$ is the initial feed volume prior to the stage and $Vol_{permeate}$ is the total volume of permeate produced in the preceding stage. This remaining volume in the feed loop after each stage can be used to find the concentration at any point in the feed loop. The remaining parameters which change for each stage such as mole fraction, molecular weight and feed solution can be determined utilizing the above information easily.

1.4. Model Assumptions

- A mean value of pore diameter and fractional void volume of the membrane was assumed and it remains constant throughout.
- For every stage of the MSVMD setup, thickness of membrane was considered to be constant along its length.
- It was assumed that neither any mass is consumed nor is it produced during the separation process.
- The heat transfer model was assumed to be 1-D.
- At the permeate side of the membrane, there was no temperature gradient as a result of the applied vacuum.
- It was assumed that the membrane module, flow pipes and feed tank were well insulated and no heat was lost through these.

1.5. Temperature polarization coefficient (TPC)

TPC is a dimensionless factor and a measure of the effects caused by temperature polarization phenomenon. The ratio of temperature drop between the bulk of hot feed solution and feed side membrane interface to the temperature gradient between the bulk of hot feed solution and the permeate sides can be referred to as temperature polarization coefficient. In other words, it is a ratio of the actual driving force in VMD mechanism to the driving force if there were no temperature polarization.

In the literature, TPC has been expressed in many different ways. The following expression was presented by Bandini et al. [39] based on VMD:

$$TPC = \frac{T_b - T_i}{T_b - T_v} \quad (14)$$

where,

T_v = Temperature on the permeate side,

According to the above expression, in a special case when T_i approaches T_b , TPC approaches zero and temperature polarization diminishes. This means that the process will only be governed by mass transfer. On the contrary, the process will be heat transfer limited only when TPC approaches unity, i.e. T_i approaches T_v . Another expression for TPC presented by Mericq et al. [40] is as follows:

$$TPC = \frac{T_i}{T_b} \quad (15)$$

According to the above expression, TPC approaches zero (maximum temperature polarization) if and only if $T_i = 0$, however, if $T_i = T_v$ temperature polarization coefficient should be zero, irrespective of the value of T_b . Hence, the above expression cannot be utilized to produce a true picture of the VMD process. Al-Asheh et al. [41] and Qtaishet et al. [42] also presented the same expression of TPC for VMD. In 2013 Asghari et al. [43] presented another expression for TPC based on VMD:

$$TPC = \frac{T_i - T_v}{T_b - T_v} \quad (16)$$

Matsuura et al. [44] also gave the same expression of TPC based on VMD. The above expression is utilized in the current study, since it agrees with TPC expression for DCMD. Table 2 presents a list of expressions for TPC of VMD given by researchers over the past years.

The membrane used in this study was made of PTFE material manufactured by GUOCHU TECHNOLOGY (Xiamen). Table 3 shows detailed specifications of the membrane unit utilized in the current study, as provided by the manufacturer.

For the 1st stage of each experiment, the required flow rate and temperature of the feed solution were set to the desired value. The system was allowed to reach a steady state condition denoted by constant reading of temperatures and flow rates. Usually, the time required for the system to achieve the steady state condition was of the order of 25 to 30 minutes. Five minutes' data was recorded for every point in a steady state condition. The key measurements taken from the experiments were the feed solution temperature value, vacuum pressure value, cooling water temperature, running time and vacuum tank drainage volume. One of the most vital measurement is the temperature of feed stream as it exits the membrane unit, which is noted from temperature gauge (TG101). For the subsequent stage, a temperature equal to the temperature of exiting feed stream from the previous stage was set and the whole process was repeated while keeping the flowrate constant as in the previous stage. Similarly, all the key measurements were recorded for each subsequent stage. An average of 3 data points was taken for each experiment.

4. Results and discussion

4.1. Numerical model validation

Experiments were conducted to determine the permeate flux of each stage in a 10-stage MSVMD setup for various feed inlet temperatures between 60 and 70 °C and feed flowrates between 1000 and 4000 L/hr. The experimental and numerical results were compared in the form of plots in Figures 6 and 7, respectively. The experimental and numerical results are represented by solid and dotted lines, respectively.

Similarly, the numerically and experimentally determined specific membrane area (SMA)/stage of the setup were compared, first for feed inlet temperatures between 60 °C and 70 °C, and then for feed flowrates ranging from 2000 L/hr to 4000 L/hr, as depicted in Figures 8 and 9, respectively.

In the graphs, there is an average deviation of less than 5%. To put it another way, the numerical and experimental results are in good accord.

4.2. Impact of process variables on cumulative permeate productivity of MSVMD

This section presents the impact of various process variables on cumulative permeate flux of an 18-stage VMD. Figure 10 (a) and (b) show the cumulative permeate productivity for an 18-stage VMD against feed solution inlet flowrate and permeate side pressure respectively, for feed temperatures ranging from 60 to 80 °C. Similarly, Figure 11 shows the permeate production plotted against feed solution inlet temperature, for feed flowrates ranging from 1000 to 4000 L/hr.

Higher feed flowrates produce higher permeate flux because the convection heat transfer coefficient is expected to rise which cause low energy loss owing to convection on the feed side. This ensures a higher permeate flux. Further, Figure 10 also depicts that the increase in permeate with the increase in feed flowrate is not linear, rather the permeate surge is abrupt initially and it gradually decreases as the feed flowrate continues to increase.

Table 3 Features of membrane unit used in current study.

Shell side parameters	Dimensions and features
Shell diameter d_s (mm)	90
Length of the membrane module (mm)	1225
Material	Acrylonitrile butadiene styrene
Fiber parameters	Dimensions and features
Total number of hollow fibers	1500
Outer dia of hollow membrane, d_o (mm)	1.6
Inner dia of hollow membrane, d_i (mm)	0.9
Membrane thickness, δ_m (mm)	0.35
Membrane pore size (μm)	0.5
Membrane porosity	45
Membrane Tortuosity	2
Material	PTFE

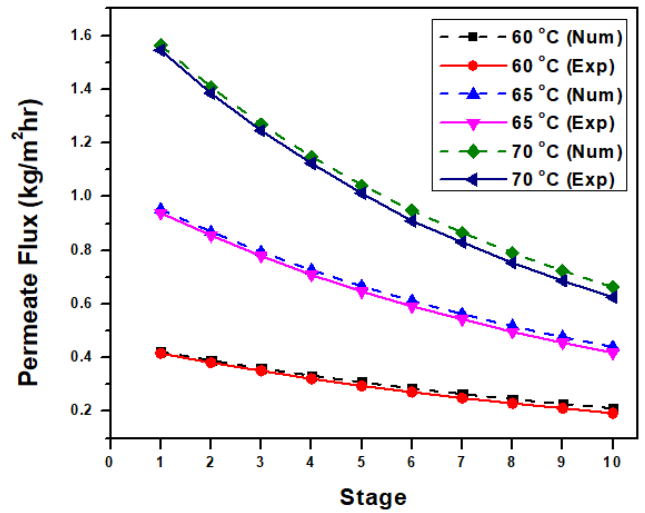


Fig. 6. Numerical and experimental results of permeate flux for feed temperature (60,65 and 70 °C) of each individual stage; Dashed lines and Solid lines represent Numerical data and Experimental data respectively.

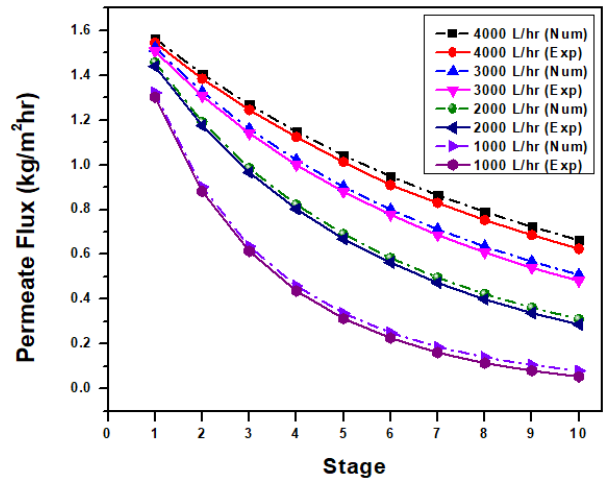


Fig. 7. Numerical and experimental permeate productivity for input flowrates (1000, 2000 and 3000 L/hr) of each individual stage; Dashed lines and Solid lines represent Numerical data and Experimental data respectively.

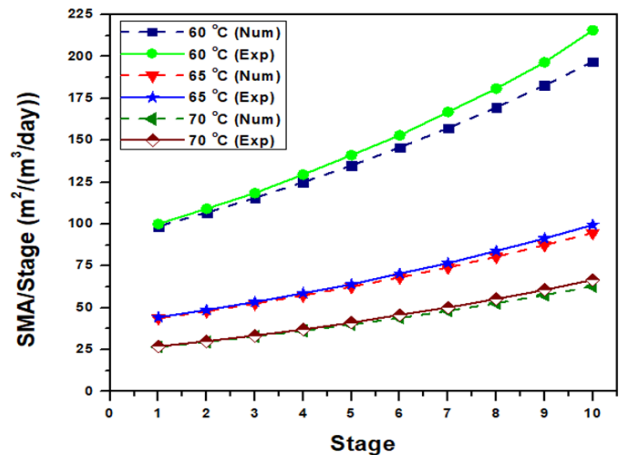


Fig. 8. Numerical and experimental SMA for each stage at feed temperature (60,65 and 70°C); Dashed lines and Solid lines represent Numerical data and Experimental data respectively.

An increasing permeate side pressure decreases the permeate output and vice versa. This is obvious, since a higher permeate pressure means a smaller vapor pressure (VP) difference across the membrane. And we know that VP difference acts as a flux driving potential in the VMD mechanism. One thing noted here is that, the nature of inverse relationship between permeate output and the vacuum pressure is almost linear.

A rise in feed solution inlet temperature brings about an upsurge in the overall permeate flux of the MSVMD setup as indicated by Figure 11 which is quite obvious due to an enhanced flux driving potential i.e. VP gradient across opposite sides of the permeable membrane, at high feed temperatures. One thing worth mentioning is that, at lower feed temperatures such as at 60 °C the difference between the overall permeate flux with varying flowrate is very small but, as the saline feed solution inlet temperature is raised, the dependence of permeate flux on the feed flowrate becomes more visible, as can be seen at $T_f = 80\text{ }^\circ\text{C}$.

4.3. Impact of process variables on cumulative TP phenomenon of MSVMD

Owing to the key role of temperature polarization (TP) phenomenon in influencing the performance of MSVMD setup, it is necessary to investigate various ways of decreasing the unwanted effects of TP, via increasing the TPC. Figure 12 (a) and (b) show the TPC for an 18-stage VMD against feed solution inlet flowrate and feed inlet bulk temperature respectively.

For a specific feed inlet temperature, a rise in feed flowrate increases the temperature polarization coefficient (TPC), which means a fall in the undesirable effect of temperature polarization. This decrease in the temperature polarization with feed flowrate is owing to the fact that, a rise in flowrate increases the convective heat transfer coefficient. Higher heat transfer coefficients cause a low temperature drop on feed side of the membrane and thus the temperature polarization phenomenon minimizes.

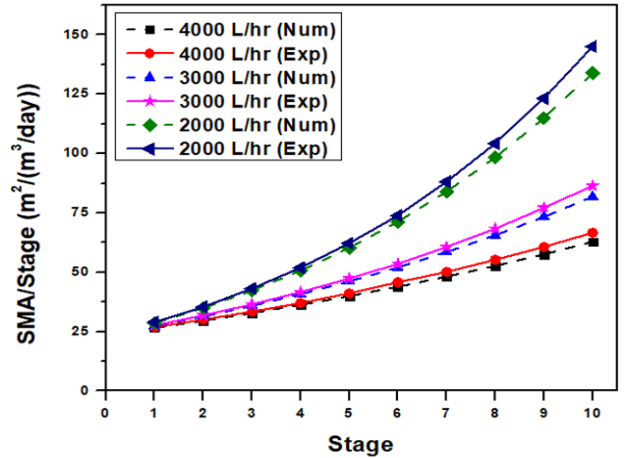


Fig. 9. Numerical and experimental SMA for individual stages at feed flowrates of 2000, 3000 and 4000 L/hr; Dashed lines and Solid lines represent Numerical data and Experimental data respectively.

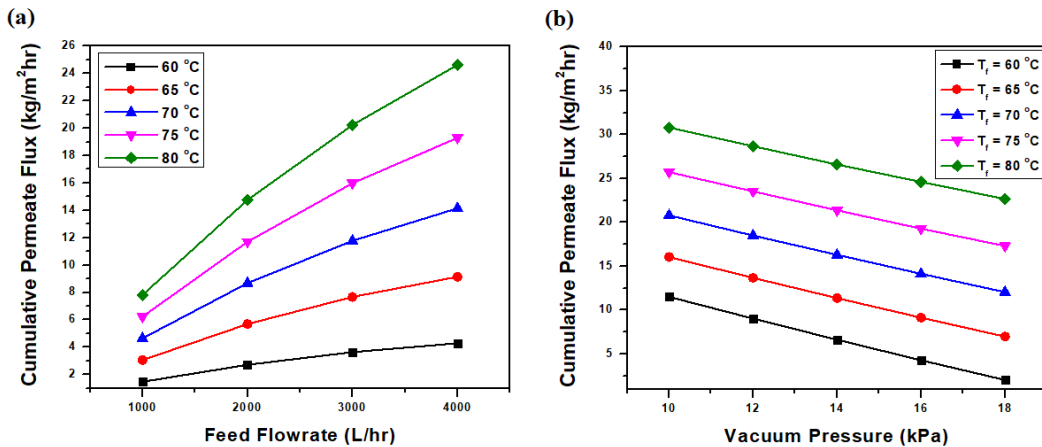


Fig. 10. Impact produced on cumulative permeate production of an 18-stage MSVMD by (a) Feed solution inlet flowrate (b) Permeate side pressure.

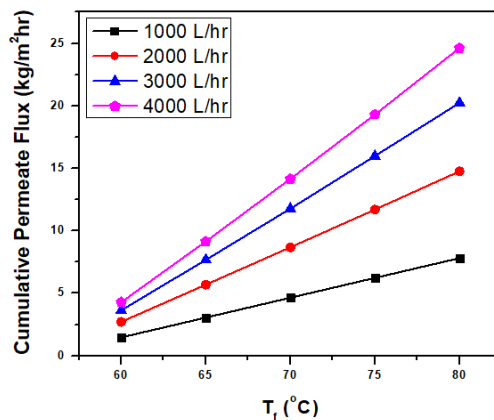


Fig. 11. Impact produced on cumulative permeate production of an 18-stage MSVMD by Feed solution inlet temperature.

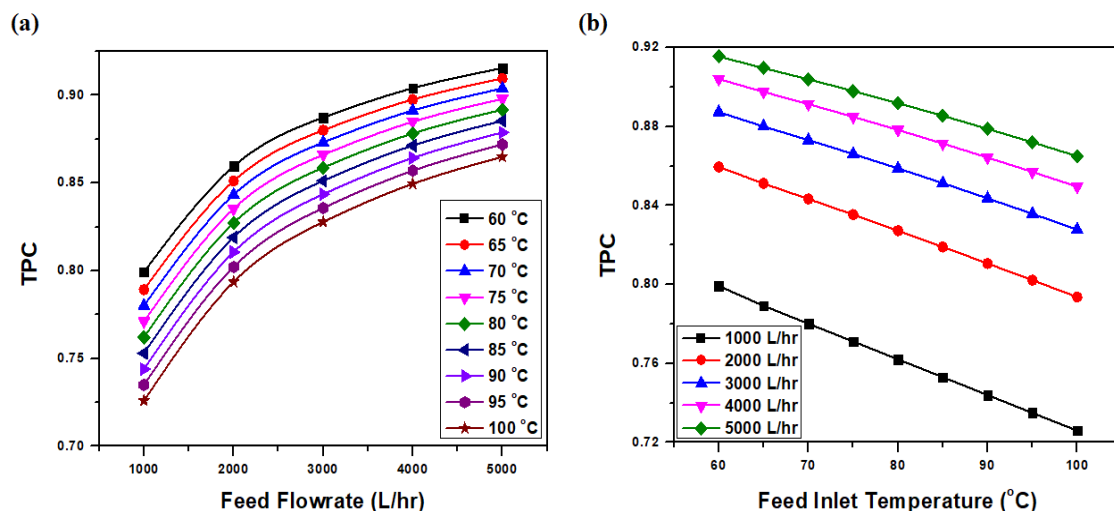


Fig. 12. Impact produced on cumulative TPC of an 18-stage MSVMD by (a) Feed solution inlet flowrate (b) Feed solution inlet temperature.

A direct relation exists between TP phenomenon and the feed solution inlet temperature. A rising TPC indicates that the temperature non-uniformity in the feed solution stream is decreasing. Thus, it is clear that at higher feed solution inlet temperatures, TPC is lower and hence the TP phenomenon is enhanced. The reason behind this behavior is that, the permeate vapors drive out a higher heat from the bulk of feed stream as they evaporate and flow inside the membrane cavities towards the vacuum side, eventually causing a higher temperature drop between the bulk of feed stream and feed side membrane interface and hence, the TPC enhances.

4.4. Simultaneous impact of membrane specifications on permeate productivity and TP phenomenon

The following section presents simultaneous impact of various membrane specifications such as number of fibers, membrane tortuosity, membrane thickness and pore size etc. on the cumulative permeate productivity and TPC of an 18-stage MSVMD setup.

Increasing the number of fibers of a hollow fiber VMD mechanism raises both its permeate flux and TPC as shown in Figure 13a. The rise in flux occurs due to rise in feed solution velocity along the membrane unit, as the feed flowrate remains the same while more fibers are added resulting in a decrease in the area for feed solution to flow. This rise in feed solution velocity increases heat transfer coefficient, ultimately causing the flux to rise. An increase in the TPC means a downfall in the undesirable effect of temperature polarization. Hence, it's clear that the number of fibers brings about a positive effect on the overall performance of the setup. Moreover, it is quite clear from the graph below that the increase in TPC with the number of fibers is independent of the feed inlet temperature. One more thing that can be concluded is that, at feed inlet temperature of 60 °C, for an additional 800 fibers in the shell, the total permeate rise is a mere 0.2808 kg/m²hr and similarly, the total TPC surge is 0.03215. This permeate and TPC rise is quite trivial as compared to the cost of additional 800 fibers, especially, if it's a small scale VMD setup.

The cumulative permeate output varies inversely with the membrane thickness as shown in Figure 13b. On the contrary, the TPC has a direct relation with the membrane thickness. So, although an increase in membrane thickness brings about a surge in the permeate output, it has also lowered the TPC which in other words mean that the undesirable effect of temperature polarization is enhanced. So, keeping in mind both the positive and the negative impacts, an optimized value of membrane thickness should be selected for the overall MSVMD performance.

As shown in Figure 13c, the impact of membrane tortuosity on the TP phenomenon and cumulative permeate productivity is quite similar. Rising tortuosity ensures lower temperature polarization, however, it also ebbtides the cumulative permeate productivity.

As shown in Figure 13d, mean pore diameter of a membrane affects the

permeate output and TPC oppositely i.e. a direct relation between the mean pore size and the permeate output is observed whereas, TPC is affected inversely by the mean pore size. This decreasing trend of TPC with the mean pore size can be described by the fact that, a higher surface area is available for water evaporation as a result of an increased mean pore size, which leads to a decrease in the membrane interface temperature and eventually enhances the undesirable effect of temperature polarization.

The permeate output, as expected, varies directly with the void volume but in case of TPC the relation is inverse as shown in Figure 13e. In other words, an increasing fractional void volume enhances the undesirable effect of temperature polarization. The reason for this inverse behavior with the TPC is that, a higher fractional void volume means the pores on the membrane are closer together and hence a high surface area is available for water evaporation eventually leading to a decrease in the membrane interface temperature.

4.5. Impact of process parameters on each individual stage of MSVMD

The analysis of overall MSVMD performance based on each individual stage is discussed in this section. It is necessary in order to determine the maximum number of stages for a specific set of conditions, that can ensure a higher permeate output while decreasing the overall cost caused by addition of stages. Figure 14 (a), (b) and (c) shows the permeate output for each individual stage of a 40-stage VMD setup, against feed solution inlet flowrate, feed inlet bulk temperature and permeate pressure respectively. For a specific feed flowrate, the decrease in permeate flux is abrupt with each subsequent stage initially, but this permeate ebbtide becomes very small for each subsequent stage after about 16 or 18 stages of the MSVMD setup. This specific behavior is more visible for a feed flowrate of 1000 L/hr. The reason behind this behavior is that in the initial stages the permeate is higher due to a higher feed solution inlet temperature and a lower salinity as compared to the following stages. A higher permeate drives out higher energy from the feed side, resulting in a decrease in the feed solution inlet temperature and an increase in the feed concentration for the successive stage.

Moreover, it can be seen that initially the individual stage permeate flux is higher for higher feed flowrates and feed inlet temperatures, and smaller permeate pressures, however, towards the final stages the permeate productivity of normally high permeate driving conditions (higher feed temperatures, flowrates and lower permeate pressures) becomes smaller as compared to lower permeate conditions (lower feed temperatures, flowrates and higher permeate pressures). In other words, the trend of higher individual permeate flux for flux promoting conditions reverses towards the final stages of MSVMD. The point at which this trend reverses is called the point of inversion. This point of inversion happens to be somewhere above 40 stages for Figure 14a,c, and 40 stages for Figure 14b. Any further addition of stages beyond this point of inversion is absolutely not recommended.

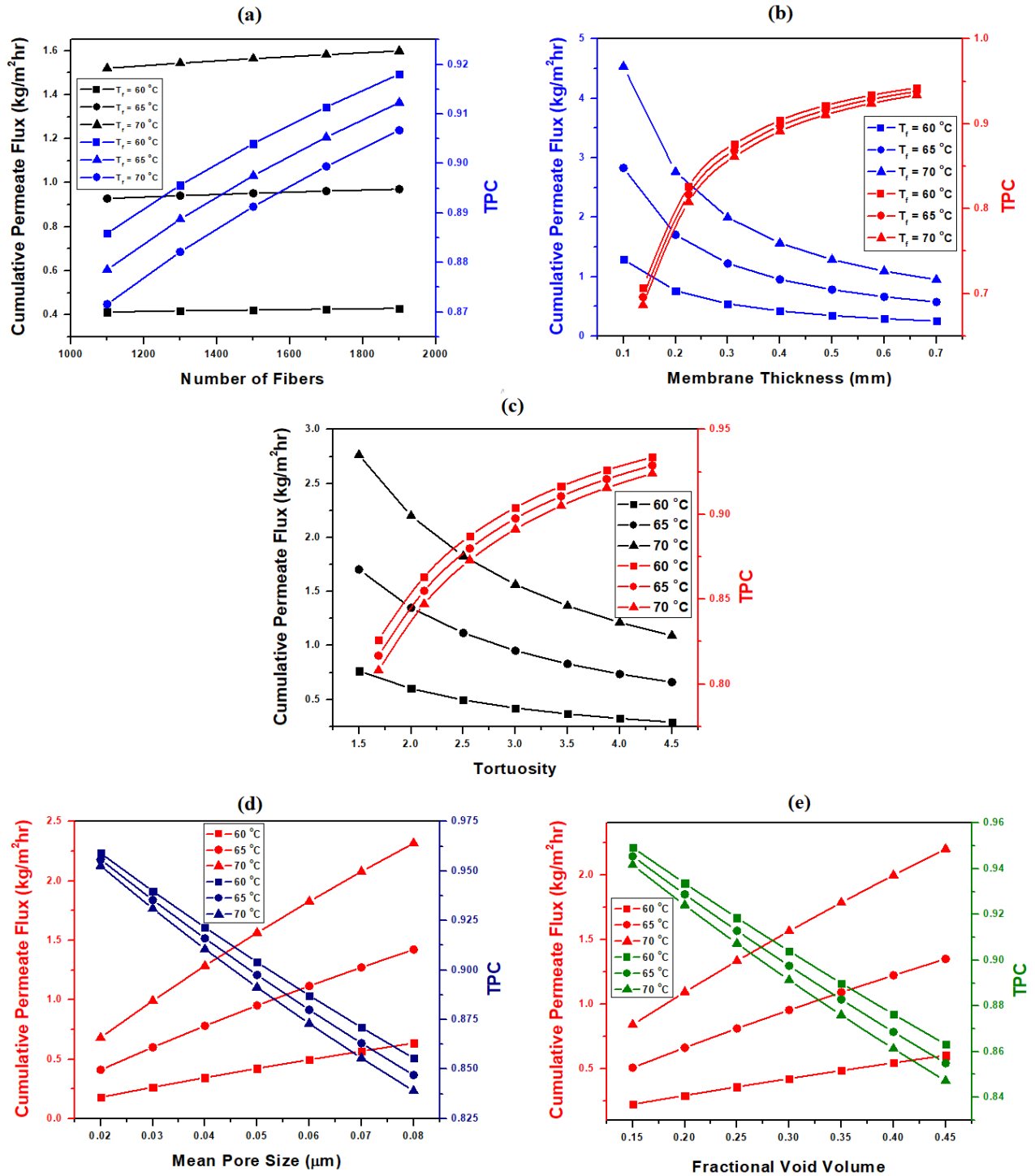


Fig. 13. Simultaneous impact of (a) Number of fibers (b) Membrane Thickness (c) Membrane Tortuosity (d) Mean Pore size (e) Fractional void volume on cumulative permeate and TPC of an 18-stage MSVMD.

4.6. Impact of membrane specifications on each individual stage of MSVMD

This section provides the impact of most prominent membrane specifications on permeate productivity of each individual MSVMD stage. Figure 15a-d show the permeate output for each individual stage of an 18-stage VMD setup, against varying membrane thickness, membrane tortuosity, mean pore size and fractional void volume respectively. The below plots suggest a similar behavior as observed for the process variables. Initially the individual stage permeate flux is higher for flux promoting

conditions (lower membrane thickness, tortuosity and higher pore size, porosity), however, towards the final stages the permeate productivity of normally high permeate driving conditions becomes smaller as compared to lower permeate conditions. The only difference is that the point of inversion arrives quite soon in case of membrane specifications as compared to the process variables. For example, for membrane thickness, membrane tortuosity and fractional void volume, the point of inversion arrives after 10 stages. Similarly, the point of inversion for mean pore size arrives after 14 stages.

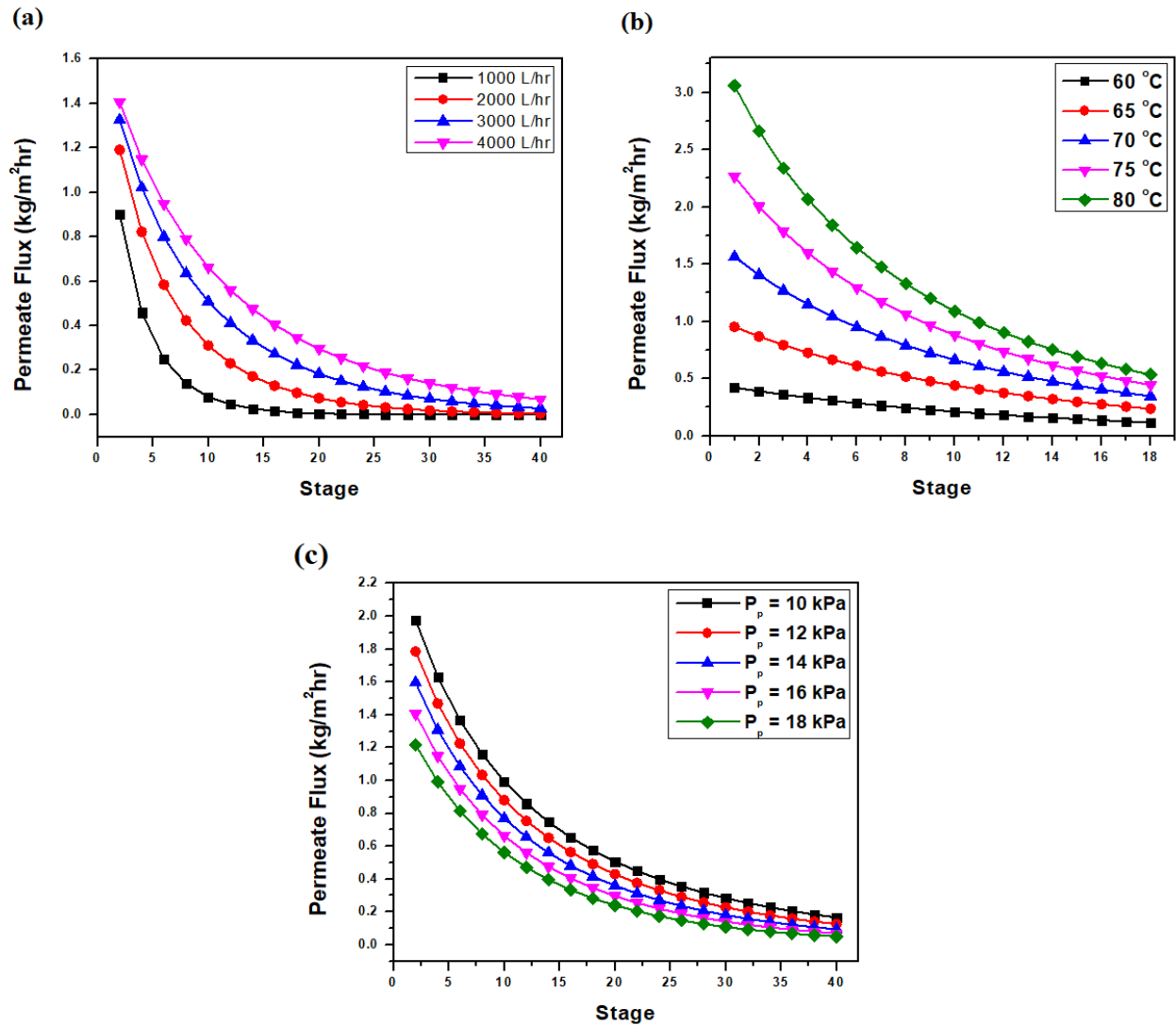


Fig. 14. Impact of (a) Feed solution inlet flowrate (b) Feed solution inlet temperature and (c) Permeate side Pressure, on individual stage permeate of a 40-stage MSVMD.

5. Conclusions

A parametric analysis of MSVMD performance was carried out in terms of cumulative permeate production and TPC. The key conclusions and results from the above study can be summarized as follows:

- At higher permeate side pressures, cumulative permeate productivity of MSVMD is reduced; however, higher values of feed solution inlet flowrate and feed solution inlet temperature ensures a higher cumulative permeate productivity.
- The cumulative TPC enhances with the rise in feed solution inlet flowrate, however, it reduces as the feed solution inlet temperature is enhanced.
- The surge in TPC with flowrate is more prominent initially, whereas it gradually diminishes at higher flowrates. TPC reduction with a corresponding rise in feed inlet temperature remains linear.
- An increase in membrane thickness and tortuosity increases TPC while lowering cumulative permeate productivity; however, mean pore size and fractional void volume have the reverse effect.
- The permeate productivity of each successive stage is lower than the predecessor stage, however, this behavior is more prominent in initial stages and fades away towards the final stages.

- The point of inversion happens to be quite higher for change in process variables (about 40 stages) as compared to membrane characteristics (below 20 stages).

The present study is a comprehensive guideline for the impact of various process variables on the cumulative permeate productivity and TPC of MSVMD. For some of the prominent process variable and membrane characteristic, an optimum range of number of stages was found for the best possible performance of MSVMD at the minimum cost.

Although this study has been carried out for VMD specifically, the idea of point of inversion is essentially applicable to multi-staging in other configurations too. The exact calculations however can be different for other configurations.

Acknowledgements:

The authors would like to thank Higher Education Commission (HEC), Govt. of Pakistan for the financial support in the form of NRP # 5550 and Ghulam Ishaq Khan Institute of Engineering Sciences and Technology for providing support during the preparation of this work.

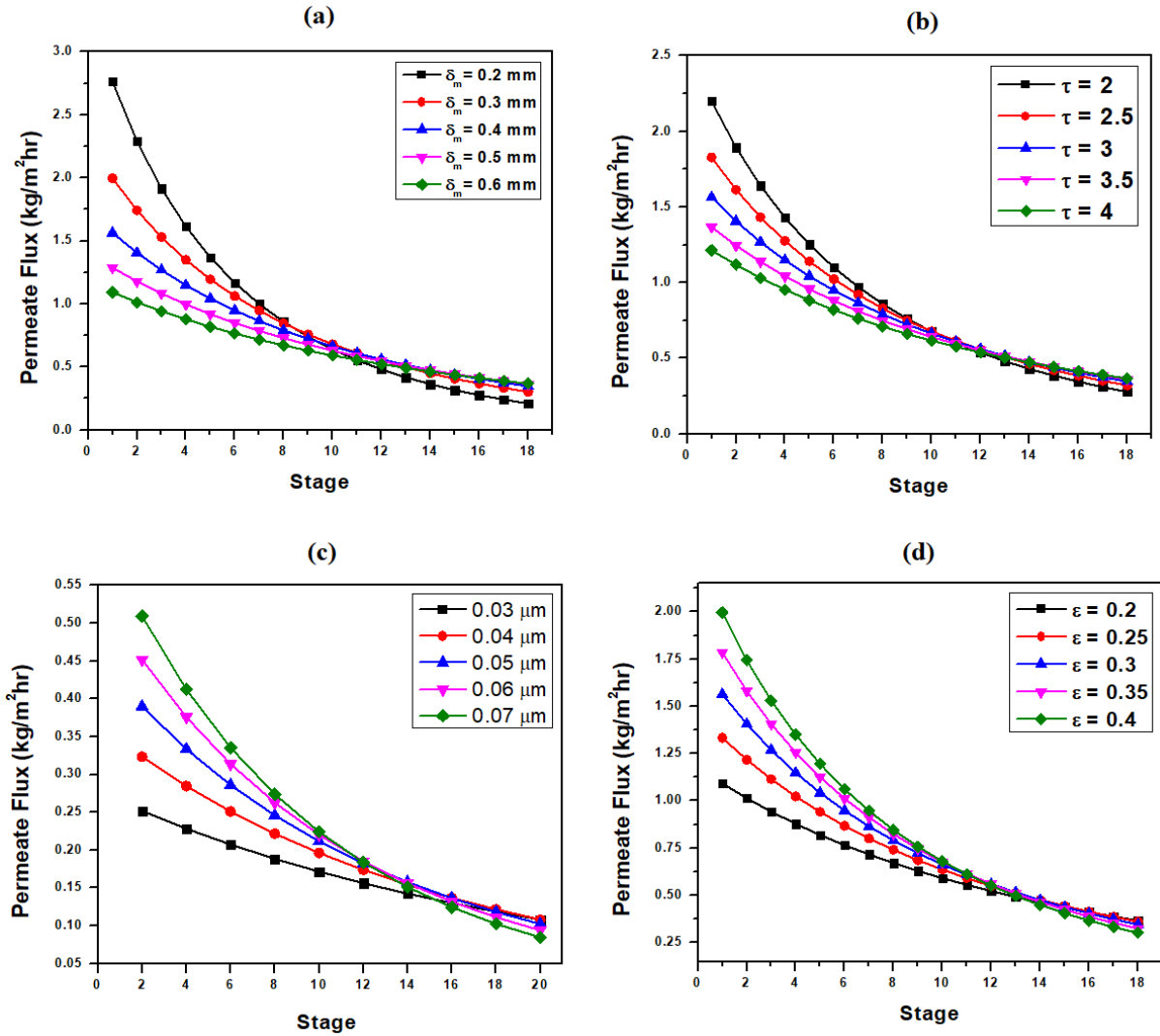


Fig. 15. Impact of (a) Membrane thickness (b) Membrane tortuosity (c) Mean pore size (d) Fractional void volume on individual stage permeate of a 40-stage MSVMD.

References

- [1] M. Elimelech, W.A. Phillip, The future of seawater desalination: Energy, technology, and the environment, *Science* (80-.). 333 (2011) 712–717. <https://doi.org/10.1126/science.1200488>.
- [2] P.H. Gleick, *The World’s Water Volume 7*, Berkeley Plan. J. 26 (2013) 217–220.
- [3] N. Ghaffour, T.M. Missimer, G.L. Amy, Technical review and evaluation of the economics of water desalination: Current and future challenges for better water supply sustainability, *Desalination*. 309 (2013) 197–207. <https://doi.org/10.1016/j.desal.2012.10.015>.
- [4] H. Ettouney, M. Wilf, Conventional Thermal Process, in: A. Cipollina, G. Micale, L. Rizzuti (Eds.), *Seawater Desalin. Conv. Renew. Energy Process.*, Springer Science & Business Media, 2009: p. 306. <https://doi.org/10.1007/978-3-642-01150-4>.
- [5] S. Al-Obaidani, E. Curcio, F. Macedonio, G. Di Profio, H. Al-Hinai, E. Drioli, Potential of membrane distillation in seawater desalination: Thermal efficiency, sensitivity study and cost estimation, *J. Memb. Sci.* 323 (2008) 85–98. <https://doi.org/10.1016/j.memsci.2008.06.006>.
- [6] R. Baghel, S. Upadhyaya, K. Singh, S.P. Chaurasia, A.B. Gupta, R.K. Dohare, A review on membrane applications and transport mechanisms in vacuum membrane distillation, *Rev. Chem. Eng.* 34 (2017) 73–106. <https://doi.org/10.1515/revce-2016-0050>.
- [7] P. Biniarz, N.T. Ardekani, M.A. Makarem, M.R. Rahimpour, Water and wastewater treatment systems by novel integrated membrane distillation (MD), *ChemEngineering*. 3 (2019) 1–36. <https://doi.org/10.3390/chemengineering3010008>.
- [8] L. Martínez, F.J. Florido-Díaz, A. Hernández, P. Prádanos, Characterisation of three hydrophobic porous membranes used in membrane distillation: Modelling and evaluation of their water vapour permeabilities, *J. Memb. Sci.* 203 (2002) 15–27. [https://doi.org/10.1016/S0376-7388\(01\)00719-0](https://doi.org/10.1016/S0376-7388(01)00719-0).
- [9] H.D. Baehr, K. Stephan, Heat conduction and mass diffusion, *Heat Mass Transf.* 108 (1998) 105–250. https://doi.org/10.1007/978-3-662-03659-4_2.
- [10] S. Zhang, L. Pu, L. Xu, R. Liu, Y. Li, Melting performance analysis of phase change materials in different finned thermal energy storage, *Appl. Therm. Eng.* 176 (2020) 115425. <https://doi.org/10.1016/j.applthermaleng.2020.115425>.
- [11] P. Pal, Arsenic Removal by Membrane Distillation, in: *Groundw. Arsen. Remediat.*, Elsevier, 2015: pp. 179–270. <https://doi.org/10.1016/b978-0-12-801281-9.00005-9>.
- [12] Handbook of Membrane Reactors | ScienceDirect, (n.d.). <https://www.sciencedirect.com/book/9780857094155/handbook-of-membrane-reactors>.
- [13] M. Essalhi, M. Khayet, Membrane Distillation (MD), in: *Prog. Filtr. Sep.*, Elsevier Ltd, 2015: pp. 61–99. <https://doi.org/10.1016/B978-0-12-384746-1.00003-3>.
- [14] A. Alkhdhiri, N. Hilal, Membrane distillation-Principles, applications, configurations, design, and implementation, in: *Emerg. Technol. Sustain. Desalin. Handb.*, Elsevier, 2018: pp. 55–106. <https://doi.org/10.1016/B978-0-12-815818-0.00003-5>.
- [15] A. Gugliuzza, A. Basile, Membrane contactors: Fundamentals, membrane materials and key operations, in: *Handb. Membr. React.*, Elsevier Ltd, 2013: pp. 54–106. <https://doi.org/10.1533/9780857097347.1.54>.
- [16] M.R. Rahimpour, N.M. Kazerooni, M. Parhoudeh, Water treatment by renewable energy-driven membrane distillation, in: *Curr. Trends Futur. Dev. Membr. Renew.*

- Energy Integr. with Membr. Oper., Elsevier, 2018: pp. 179–211. <https://doi.org/10.1016/B978-0-12-813545-7.00008-8>.
- [17] Y.D. Kim, W.S. Kim, Experimental and theoretical investigations of a novel multi-stage direct contact membrane distillation module, in: Proc. World Congr. New Technol., 2016. <https://doi.org/10.11159/icepr16.151>.
- [18] A. Omar, A. Nashed, R. Taylor, Single Vs Multi-Stage Vacuum Membrane Distillation: an Energetic Analysis, in: Unsworks.Unsw.Edu.Au, 2018: p. 11. <http://unsworks.unsw.edu.au/fapi/datastream/unsworks:51215/binc63b546d-3329-46c7-ab51-ff8d664e361f?view=true> (accessed October 7, 2020).
- [19] E. Jang, S.H. Nam, T.M. Hwang, S. Lee, Y. Choi, Effect of operating parameters on temperature and concentration polarization in vacuum membrane distillation process, Desalin. Water Treat. 54 (2015) 871–880. <https://doi.org/10.1080/19443994.2014.952673>.
- [20] A.S. Alsaadi, A. Alpatova, J.G. Lee, L. Francis, N. Ghaffour, Flashed-feed VMD configuration as a novel method for eliminating temperature polarization effect and enhancing water vapor flux, J. Memb. Sci. 563 (2018) 175–182. <https://doi.org/10.1016/j.memsci.2018.05.060>.
- [21] J. Gilron, L. Song, K.K. Sirkar, Design for cascade of crossflow direct contact membrane distillation, Ind. Eng. Chem. Res. 46 (2007) 2324–2334. <https://doi.org/10.1021/ie060999k>.
- [22] F. He, J. Gilron, K.K. Sirkar, High water recovery in direct contact membrane distillation using a series of cascades, Desalination. 323 (2013) 48–54. <https://doi.org/10.1016/j.desal.2012.08.006>.
- [23] Y. Lu, J. Chen, Optimal design of multistage membrane distillation systems for water purification, Ind. Eng. Chem. Res. 50 (2011) 7345–7354. <https://doi.org/10.1021/ie1016877>.
- [24] S.M. Shim, J.G. Lee, W.S. Kim, Performance simulation of a multi-VMD desalination process including the recycle flow, Desalination. 338 (2014) 39–48. <https://doi.org/10.1016/j.desal.2013.12.009>.
- [25] E.K. Summers, J.H. Lienhard, V. Presenter, Cycle Performance of Multi-Stage Vacuum Membrane Distillation (Ms-Vmd) Systems, in: Mit.Edu, 2013.
- [26] H.W. Chung, J. Swaminathan, D.M. Warsinger, J.H. Lienhard V, Multistage vacuum membrane distillation (MSVMD) systems for high salinity applications, J. Memb. Sci. 497 (2016) 128–141. <https://doi.org/10.1016/j.memsci.2015.09.009>.
- [27] K. Zhao, W. Heinzl, M. Wenzel, S. Büttner, F. Bollen, G. Lange, S. Heinzl, N. Sarda, Experimental study of the memsys vacuum-multi-effect-membrane-distillation (V-MEMD) module, Desalination. 323 (2013) 150–160. <https://doi.org/10.1016/j.desal.2012.12.003>.
- [28] F.H. Choo, M.K. Ja, K. Zhao, A. Chakraborty, E.T.M. Dass, M. Prabu, B. Li, S. Dubey, Experimental study on the performance of membrane based multieffect dehumidifier regenerator powered by solar energy, Energy Procedia. 48 (2014) 535–542. <https://doi.org/10.1016/j.egypro.2014.02.063>.
- [29] A. Omar, A. Nashed, Q. Li, R.A. Taylor, Experimental and numerical evaluation of the energy requirement of multi-stage vacuum membrane distillation designs, Sep. Purif. Technol. 257 (2021). <https://doi.org/10.1016/j.seppur.2020.117303>.
- [30] P. Boutikos, E.S. Mohamed, E. Mathioulakis, V. Belessiotis, A theoretical approach of a vacuum multi-effect membrane distillation system, Desalination. 422 (2017) 25–41. <https://doi.org/10.1016/j.desal.2017.08.007>.
- [31] R. Lefers, N.M.S. Bettahalli, N. Fedoroff, S.P. Nunes, T.O. Leiknes, Vacuum membrane distillation of liquid desiccants utilizing hollow fiber membranes, Sep. Purif. Technol. 199 (2018) 57–63. <https://doi.org/10.1016/j.seppur.2018.01.042>.
- [32] N. Hoda, S. V. Suggala, P.K. Bhattacharya, Pervaporation of hydrazine-water through hollow fiber module: Modeling and simulation, Comput. Chem. Eng. 30 (2005) 202–214. <https://doi.org/10.1016/j.compchemeng.2005.08.014>.
- [33] L.H. Cheng, P.C. Wu, J. Chen, Modeling and optimization of hollow fiber DCMD module for desalination, J. Memb. Sci. 318 (2008) 154–166. <https://doi.org/10.1016/j.memsci.2008.02.065>.
- [34] G. Ramon, Y. Agnon, C. Dosoretz, Heat transfer in vacuum membrane distillation: Effect of velocity slip, J. Memb. Sci. 331 (2009) 117–125. <https://doi.org/10.1016/j.memsci.2009.01.022>.
- [35] G.S. Kim, T. Cao, Y. Hwang, Thermoeconomic investigation for a multi-stage solar-thermal vacuum membrane distillation system for coastal cities, Desalination. 498 (2021). <https://doi.org/10.1016/j.desal.2020.114797>.
- [36] H.G. Grohn, 82 Influence of the Yaw Angle on Heat Transfer and Pressure Drop of Helical Type Heat Exchangers, 1988.
- [37] J. Liu, C. Wu, X. Lü, Heat and mass transfer in vacuum membrane distillation, Huagong Xuebao/CIESC J. 62 (2011) 908–915.
- [38] A.S. Alsaadi, N. Ghaffour, J.D. Li, S. Gray, L. Francis, H. Maab, G.L. Amy, Modeling of air-gap membrane distillation process: A theoretical and experimental study, J. Memb. Sci. 445 (2013) 53–65. <https://doi.org/10.1016/j.memsci.2013.05.049>.
- [39] S. Bandini, G.C. Sarti, C. Gostoli, Vacuum membrane distillation: pervaporation through porous hydrophobic membranes, in: Proc. 3rd Int. Conf. Pervaporation Chem. Ind. Nancy, Sept. 19–22, 1988: pp. 117–126.
- [40] J.P. Mericq, S. Laborie, C. Cabassud, Response to the letter-to-the-editor entitled Comments on “Evaluation of systems coupling vacuum membrane distillation and solar energy for seawater desalination,” Chem. Eng. J. 178 (2011) 477–478. <https://doi.org/10.1016/j.cej.2011.09.120>.
- [41] F. Banat, S. Al-Asheh, M. Qtaishat, Treatment of waters colored with methylene blue dye by vacuum membrane distillation, Desalination. 174 (2005) 87–96. <https://doi.org/10.1016/j.desal.2004.09.004>.
- [42] S. Al-Asheh, F. Banat, M. Qtaishat, M.Y. El-Khateeb, Concentration of sucrose solutions via vacuum membrane distillation, Desalination. 195 (2006) 60–68. <https://doi.org/10.1016/j.desal.2005.10.036>.
- [43] S.G. Lovineh, M. Asghari, B. Rajaei, Numerical simulation and theoretical study on simultaneous effects of operating parameters in vacuum membrane distillation, Desalination. 314 (2013) 59–66. <https://doi.org/10.1016/j.desal.2013.01.005>.
- [44] M. Khayet, T. Matsuura, Pervaporation and vacuum membrane distillation processes: Modeling and experiments, AIChE J. 50 (2004) 1697–1712. <https://doi.org/10.1002/aic.10161>.
- [45] S. Bandini, C. Gostoli, G.C. Sarti, Separation efficiency in vacuum membrane distillation, J. Memb. Sci. 73 (1992) 217–229. [https://doi.org/10.1016/0376-7388\(92\)80131-3](https://doi.org/10.1016/0376-7388(92)80131-3).
- [46] M.H. Sharqawy, J.H. Lienhard V, S.M. Zubair, Thermophysical properties of seawater: A review of existing correlations and data, Desalin. Water Treat. 16 (2010) 354–380. <https://doi.org/10.5004/dwt.2010.1079>.